arXiv:1912.05405v1 [cs.CV] 11 Dec 2019

Training Deep SLAM on Single Frames

Igor Slinko, Anna Vorontsova, Dmitry Zhukov, Olga Barinova, Anton Konushin
Samsung AI Center Russia, Moscow
{i.slynko,a.vorontsova,d.zhukov,o.barinova,a.konushin}@samsung.com

Abstract

Learning-based visual odometry and SLAM methods demonstrate a steady improvement over past years. However, collecting ground truth poses to train these methods is difficult and expensive. This could be resolved by training in an unsupervised mode, but there is still a large gap between performance of unsupervised and supervised methods. In this work, we focus on generating synthetic data for deep learning-based visual odometry and SLAM methods that take optical flow as an input. We produce training data in a form of optical flow that corresponds to arbitrary camera movement between a real frame and a virtual frame. For synthesizing data we use depth maps either produced by a depth sensor or estimated from stereo pair. We train visual odometry model on synthetic data and do not use ground truth poses hence this model can be considered unsupervised. Also it can be classified as monocular as we do not use depth maps on inference.

We also propose a simple way to convert any visual odometry model into a SLAM method based on frame matching and graph optimization. We demonstrate that both the synthetically-trained visual odometry model and the proposed SLAM method build upon this model yields state-of-the-art results among unsupervised methods on KITTI dataset and shows promising results on a challenging EuRoC dataset.

1. Introduction

Simultaneous localization and mapping is an essential part of robotics and augmented reality systems. Deep learning-based methods for visual odometry and SLAM [32, 33, 41, 14, 35] have evolved over the last years and are able to compete with classical geometry-based methods on the datasets with predominant motions along plain surfaces like KITTI[12] and Malaga[3].

However, the practical use of deep learning-based methods for visual odometry and SLAM is limited by the difficulty of acquiring precise ground truth camera poses. To overcome this problem, unsupervised visual odometry methods are being actively investigated [1, 11, 38, 17, 36].

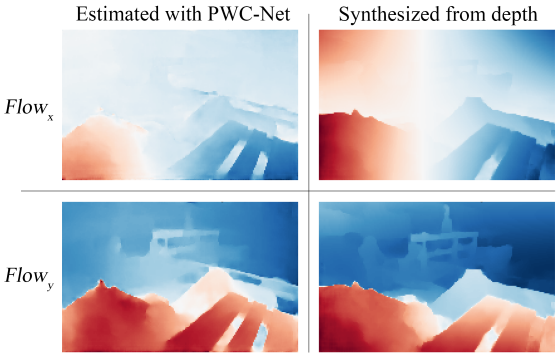


Figure 1: Optical flow estimated with trainable method (PWC-Net) on consecutive frames against the one synthesized from depth map and given 6DoF.

Existing methods [41, 42, 29, 31, 2] use video sequences for training. They estimate camera movements and depth maps jointly. For a pair of consecutive frames, the first frame is re-rendered from the point of view of the second one. The difference between re-rendered first frame and ground truth second frame is used in a loss function.

We propose an alternative approach, that requires only individual frames with depth rather than video sequences. In our approach, we sample random camera motions with respect to the physical motion model of an agent. Then for each sampled camera motion we synthesize corresponding optical flow between a real frame and a virtual frame. The resulting synthesized optical flow with generated ground truth camera motions can be used for training a learning-based visual odometry model.

Our contribution is twofold:

- First, we introduce an unsupervised method of training visual odometry and SLAM models on synthetic optical flow generated from depth map and arbitrary camera movement between selected real frame and virtual frame. This approach does not use frame sequences for training and does not require ground truth camera poses.
- Second, we propose a simple way to convert any vi-

sual odometry model into a SLAM system with frame matching and graph optimization.

We demonstrate that our approach outperforms state-of-the-art unsupervised deep SLAM methods on KITTI dataset. Also we tried our method on challenging EuRoC dataset, and to the best of our knowledge, this is the first unsupervised learnable method ever evaluated on EuRoC.

2. Related work

2.1. Classical methods

Several different mathematical formulations for visual odometry have been considered in the literature. Geometry-based visual odometry methods can be classified into direct (*e.g.* [15]) and indirect (*e.g.* [24]) or dense (*e.g.* [27]) and sparse (*e.g.* [10]).

Direct methods take original images as inputs, while indirect methods process detected keypoints and corresponding features. Dense methods accept regular inputs such as images, optical flow or dense feature representations. In sparse methods, data of irregular structure is used.

Many of the classical works apply bundle adjustment or pose graph optimization in order to mitigate the odometry drift. Since this strategy showed its effectiveness in related tasks [24, 25], we adopt it in our deep learning-based approach.

2.2. Supervised learning-based methods

DeepVO [32] was a pioneer work to use deep learning for visual odometry. This deep recurrent network regresses camera motion using pretrained FlowNet [9] as a feature extractor. ESP-VO [34] extends this model with sequence-to-sequence learning and introduces an additional loss on global poses. LS-VO [7] also uses the result of FlowNet and formulates the problem of estimating camera motion as finding a low-dimensional subspace of the optical flow space. DeMoN [30] estimates both camera motion, optical flow and depth in the EM-like iterative network. By efficient usage of consecutive frames, DeMoN improves accuracy of depth prediction over single-view methods. This work became a basis for the first deep SLAM method called DeepTAM [41]. Similar ideas were implemented in ENG [8], which was proved to work on both indoor and outdoor datasets.

2.3. Unsupervised learning-based methods

Recent advances in simultaneous depth and motion estimation [41] [29] from video sequences allow to track more accurate camera position in an unsupervised manner. These methods exploit sequential nature of the data in order to model scene dynamics and take clues from occlusion, between-frame optical flow consistency and other factors ([42], [13], [31]). To achieve motion consistency, additional modalities of data such as depth maps are estimated in a joint pipeline. Similarly to these approaches, we use depth maps; however, we once estimate depth maps from a stereo pair, and keep them unchanged during optical flow synthesis.

2.4. Novel view synthesis

The idea of novel view synthesis using single frame or stereo pair and optical flow has been exploited in [41] . In this method, model is trained in a supervised manner by minimizing difference between estimated and ground truth camera poses. Novel view synthesis is used as a part of working pipeline, with new camera position predicted, virtual frame synthesized, and movement between virtual and current frame estimated. Therefore, this method operates mainly in the image domain, utilizing optical flow only to transit between different image instances. In our approach, we synthesize optical flow rather than images. We also generate training data only on training stage, and do not use it during inference.

3. Proposed method

3.1. Visual odometry model

For visual odometry, we adopt a neural network from [26] that estimates relative rotation and translation in form of 6DoF from dense optical flow. The model architecture is shown on Figure 2. Generally speaking. our approach can be applied to any model that takes optical flow as an input and predicts 6DoF.

We use PWC-Net [28] for optical flow estimation. The source code and pretrained weights are taken from the official repository [1]. For KITTI, we opted for weights pretrained on FlyingThings3D [22] dataset and fine-tuned on KITTI optical flow dataset[23]. For EuRoC, which is in grayscale, we fine-tuned PWC-Net weights and using Sintel dataset [5] converted to grayscale.

In our experiments, we found out that a single neural network can effectively handle motions within a certain range. However, motions between the first and the last frames in loops differ significantly from motions between consecutive frames: not only are they of different scale but also much more diverse. To address this problem, we train two models: NN_{cons} model to estimate motions between consecutive frames and NN_{loops} to predict motions specifically between the first and the last frames in a loop.

3.2. Synthetic training data generation

Taking depth map and an arbitrary motion in form of 6DoF, the method runs as follows:

[1] https://github.com/NVlabs/PWC-Net

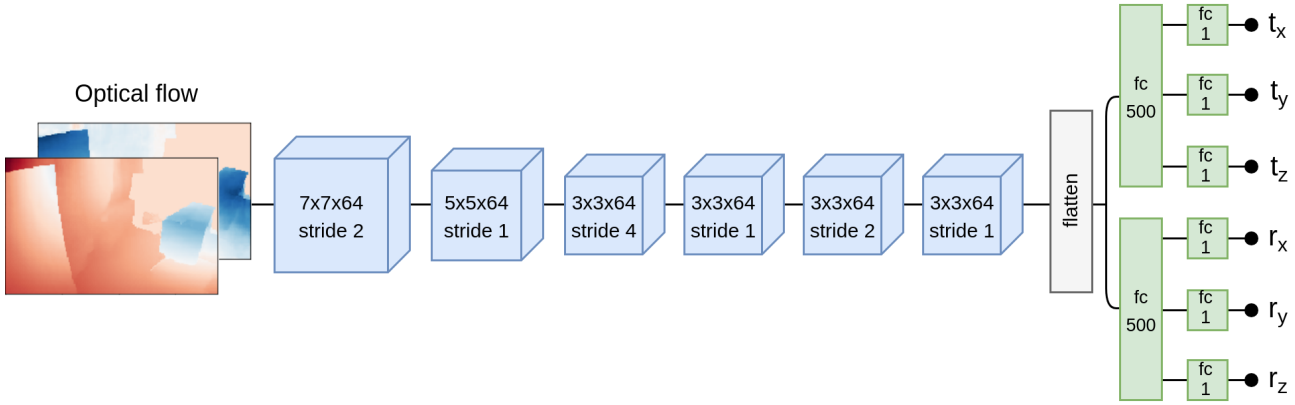


Figure 2: Architecture of visual odometry model

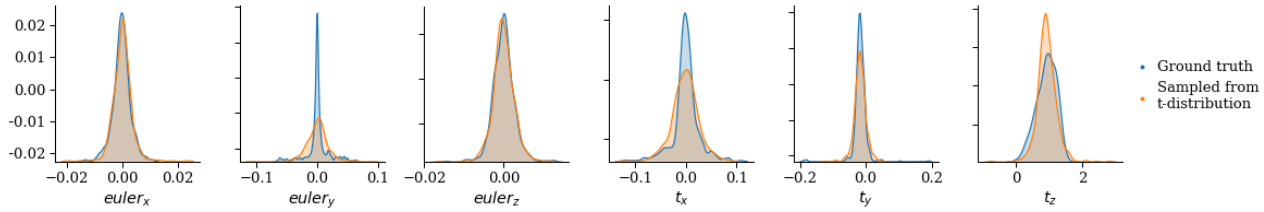


Figure 3: Distribution of 6DoF motion in KITTI dataset

1. First, we map depth map pixels into points in a frustum that gives a point cloud.

2. To build a virtual point cloud, we represent motion in form of SE3 matrix and apply it to the current point cloud, obtaining this point cloud from another view point.

3. Next, we re-project this virtual point cloud back to image plane, that gives shifted pixel grid.

4. To get absolute values of optical flow, we calculate the difference between re-projection and regular pixel grid of a source depth map.

Then, this newly synthesized optical flow can be used as an input to a visual odometry network.

The camera movements should be generated with taking physical motion model of an agent into account. Since existing datasets do not contain such information, we estimate the motion model from the ground truth data. By modelling, we approximate ground truth distribution of 6DoF using Student's t-distribution Figure 3. We adjust the parameters of this distribution once and keep them fixed during training, while 6DoF are being sampled randomly.

In case that dataset does not contain depth maps, they can be estimated from a monocular image or a stereo pair. In our experiments, we obtain depth z from disparity d similar to [37].

$$z = \frac{fB}{d}, \tag{1}$$

where f is focal length and B is distance between stereo cameras.

To estimate disparity, we match left and right image with the same PWC-Net [28] as was used to estimate optical flow.

Since we do not need ground truth camera poses for data synthesis, the proposed approach can be considered unsupervised.

3.3. Relocalization

Relocalization can be reformulated as image retrieval task Figure 4. Following a standard approach, we measure distance between frames according to their visual similarity. Here, we use classical Bag of Visual Words (BoVW) from OpenCV library [4] that is applied to SIFT features [19]. These features are stored in a database. To create a topological map, for each new frame its 20 nearest neighbors are extracted from database. These found frames are further filtered by applying Lowe's ratio test [18] and rejecting candidates with less then N_{th} matched keypoints.

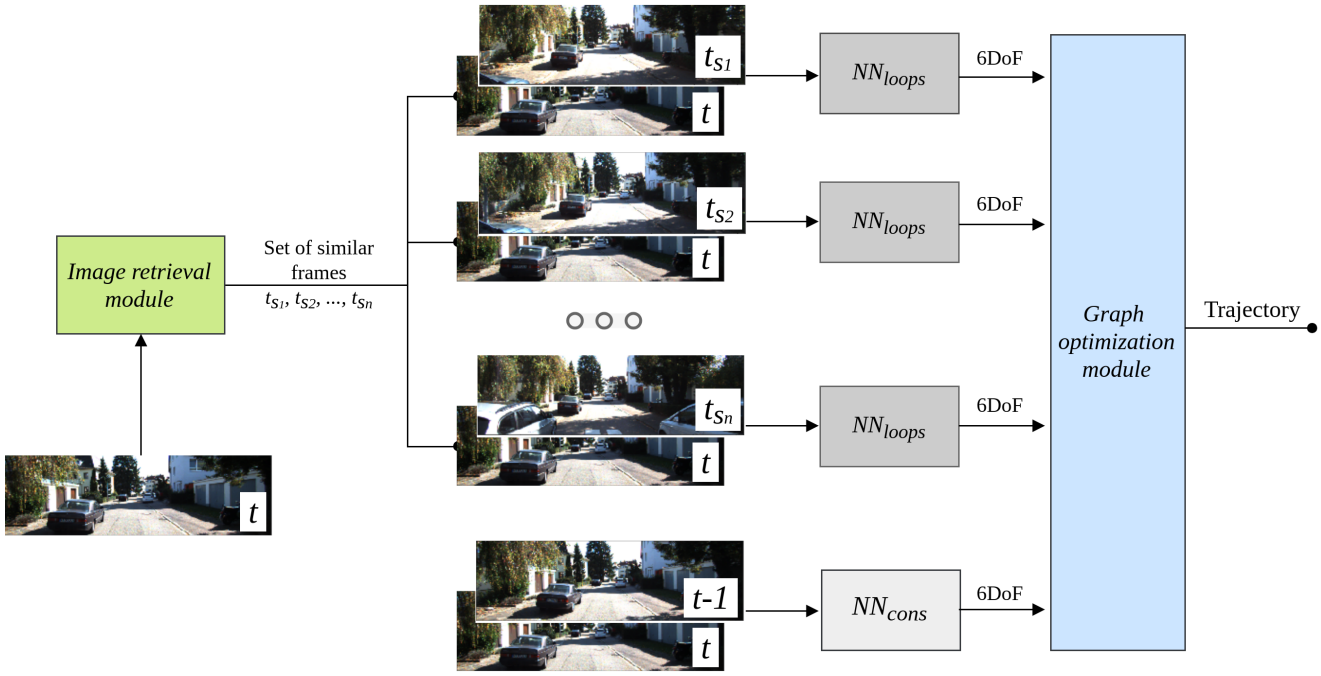


Figure 4: Architecture of proposed SLAM method

3.4. Graph optimization

We adopt graph optimization in order to expand a visual odometry method to a SLAM algorithm. One way to formulate SLAM is to use a graph with nodes corresponding to the camera poses and edges representing constraints between these poses. Two camera poses are connected with an edge if they correspond to consecutive frames or if they are considered similar by relocalization module. The edge constraints are obtained as relative motions predicted with visual odometry module. Once such a graph is constructed, it can be further optimized in order to find the spatial configuration of the nodes that is the most consistent with the relative motions modeled by the edges. The nodes obtained through optimization procedure are then used as final pose estimates. The reported metrics are thus computed by comparing these estimates with ground truth poses.

We opted for a publicly available g2o library [16] that implements least-squares error minimization. To incorporate optimization module in our Python-based pipeline we use Python binding for g2o [2].

The interaction between visual odometry networks NN_{cons}, NN_{loops} and graph optimization module is guided by a set of hyperparameters:

- C_{s_i} – coefficient for standard deviation
- C_r – extra scaling factor for rotation component
- T_{loop} – loop threshold: a loop is detected if difference between indices of two images exceeds given threshold. In this case, relative motion is predicted using loop network NN_{loops}, otherwise NN_{cons} is used.

We adjust these hyperparameters on a validation subset and then evaluate our method on a test subset.

To construct a graph, we need to pass 7×7 information matrix P_i corresponding to 3D translation vector and rotation in form of a quaternion.

First, we compose resulting covariance matrix as:

$$Q_i = C_{s_i} \begin{bmatrix} \sigma^2_{t_x} & 0 & 0 & 0 & 0 & 0 \\ 0 & \sigma^2_{t_y} & 0 & 0 & 0 & 0 \\ 0 & 0 & \sigma^2_{t_z} & 0 & 0 & 0 \\ 0 & 0 & 0 & C_r\sigma^2_{\alpha} & 0 & 0 \\ 0 & 0 & 0 & 0 & C_r\sigma^2_{\beta} & 0 \\ 0 & 0 & 0 & 0 & 0 & C_r\sigma^2_{\gamma} \end{bmatrix} \quad (2)$$

where α, β, γ stand for Euler angles $euler_x$, $euler_y$, $euler_z$ respectively.

A conversion between this matrix and Q_i is performed according to [6]:

$$P_i = \left(\frac{\partial p_7(p_6)}{\partial p_6} Q_i \frac{\partial p_7(p_6)}{\partial p_6} \right)^{-1} \quad (3)$$

[2] https://github.com/uoip/g2opy

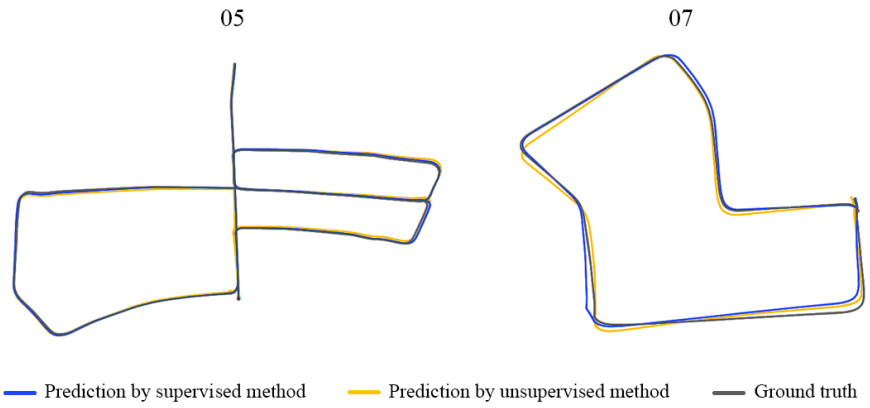


Figure 5: Ground truth and estimated KITTI trajectories

4. Experiments

4.1. Datasets

KITTI odometry 2012. We used KITTI dataset to evaluate our method in a simple scenario. We trained on trajectories 00, 02, 08 and 09 and tested on trajectories 03, 04, 05, 06, 07, 10.

It is worth noting that ground truth poses were collected using GPS sensor that yielded noisy measurements of motion along y-axis (there are vertical movements perpendicular to the surface of the road). This effect is cumulative: while relative motion between consecutive frames was measured quite precisely, the difference in absolute height between the first and the last frame of a loop may be up to 2 meters.

EuRoC. This dataset was recorded using flying drone in two different environments. 6DoF ground truth poses are captured by laser tracker or motion capture system depending on environment. The sensor and ground truth data are calibrated and temporally aligned, with all extrinsic and intrinsic calibration parameters provided. As original frames come unrectified, preprocessing included removing distortion. We validated on trajectories MH_02_easy, V1_02_medium and tested on V1_03_difficult and V2_03_difficult, while other trajectories were used for training.

Due to complexity of the environment, dynamic motions and weakly correlated, entangled trajectories, EuRoC appears to be a challenging task for trainable methods. Moreover, images are in grayscale, that adds difficulty for methods that match pixels based on their color rather than pure intensity. To the best of our knowledge, we present the first trainable method that demonstrates competitive results on EuRoC among all methods trained in an unsupervised manner.

Method	ATE	t_{err}	r_{err}
NN_{cons}	4.38 ± 0.36	2.07 ± 0.03	0.93 ± 0.04
NN_{loops}	9.33 ± 1.04	3.15 ± 0.12	1.42 ± 0.03
SLAM	1.84 ± 0.06	1.54 ± 0.04	0.74 ± 0.04

Table 1: Results of supervised visual odometry models and SLAM method on KITTI dataset. Optimal parameters for SLAM are $C_{s_i} = 10000$, $C_r = 1$, $T_{loop} = 50$

Method	ATE	t_{err}	r_{err}
NN_{cons}	14.30 ± 1.57	5.57 ± 0.33	2.23 ± 0.15
NN_{loops}	16.21 ± 1.42	6.43 ± 0.23	2.82 ± 0.10
SLAM	3.24 ± 0.17	3.37 ± 0.12	1.24 ± 0.04

Table 2: Results of unsupervised visual odometry models and SLAM method on KITTI dataset. Optimal parameters for SLAM are $C_{s_i} = 10000$, $C_r = 0.004$, $T_{loop} = 50$

Method	t_{err}	r_{err}
ORB-SLAM2[24]	2.41	**0.245**
Ours, SLAM	**1.54**	0.74

Table 3: Metrics on KITTI for supervised methods. Numbers are taken from [39]

4.2. Training procedure

The visual odometry model is trained from scratch using Adam optimization algorithm with amsgrad option switched on. The batch size is set to 128, the momentum is fixed to (0.9, 0.999).

In our experiments, we noticed that despite loss being almost constant among several re-runs, final metrics (ATE, RPE etc.) may fluctuate significantly. This spreading is

Method	ATE	t_{err}	r_{err}
SfMLearner[42]	28.14	12.21	4.74
Depth-VO-Feat[38]	16.83	8.15	4.00
SC-SfMLearner[2]	17.92	7.42	3.35
UnDeepVO[17]		6.27	3.39
GeoNet[36]		13.12	7.38
Vid2Depth[21]		37.98	18.24
SGANVO[11]		5.12	2.53
Ours, VO	14.30	5.57	2.23
Ours, SLAM	**3.24**	**3.37**	**1.24**

Table 4: Metrics on KITTI for unsupervised methods. Numbers are taken from [39]

assumed to be caused by optimization algorithm terminating at different local minima depending on weights initialization and randomness incorporated by sampling batches. We address this challenge by adopting learning rate schedule in order to force optimization algorithm to traverse several local minima during the training process. Switching our training procedure for cyclic learning rate helped to decrease standard deviation of final metrics and the values of metrics themselves.

Initially, values of learning rate are bounded by [0.0001, 0.001]. In addition, if validation loss does not improve for 10 epochs, both the lower and upper bounds are multiplied by 0.5. Training process is terminated when learning rate becomes negligibly small. We used 10^{-5} as a learning rate threshold. Under these conditions, models are typically trained for about 80 epochs.

In several papers on trainable visual odometry [7, 20, 32, 40, 41], different weights are used for translation loss and rotation loss. Since small rotation errors may have a crucial impact on the shape of trajectory, precise estimation of Euler angles is more important compared to translations. We multiply loss for rotation components by 50, as it was proposed in [7].

4.3. Evaluation protocol

We evaluate visual odometry methods with several commonly used metrics.

For KITTI, we follow the evaluation protocol implemented in KITTI devkit [3] that computes translation (t_{err}) and rotation (r_{err}) errors. Both translation and rotation errors are calculated as root-mean-squared-error for all possible sub-sequences of length (100, ..., 800) meters. The metrics reported are the average values of these errors per 100 meters.

For EuRoC, we use RPE metric that measures frame-to-frame relative pose error.

[3] https://github.com/alexkreimer/odometry/devkit

To provide a detailed analysis, we also report values of absolute trajectory error (ATE), that measures the average pairwise distance between predicted and ground truth camera poses.

Since the results between different runs vary significantly, in order to obtain fair results we conduct all experiments for 5 times with different random seeds. The metrics reported are mean and standard deviation of execution results.

4.4. Results on KITTI

The results of our supervised and unsupervised visual odometry and SLAM are listed in Tab. 1 and Tab. 2, respectively. According to them, visual odometry network NN_{cons} trained on consecutive frames yields better results comparing to NN_{loops} trained to estimate targets coming from a wider distribution. Combination of these two networks within a deep SLAM architecture helps to improve accuracy of predictions significantly.

The existing quality gap between supervised and unsupervised approaches can be explained by non-rigidity of the scene, that exceeds the limitations of our data generation method. To obtain synthetic optical flow, a combination of translation and rotation is applied to a point cloud. Since it does not affect pairwise distances between points, the shapes of objects presenting in the scene remain unchanged and no new points appear. Thereby, rigidity of the scene is implicitly incorporated into the data synthesizing pipeline. For KITTI, scene does not meet these requirements due to the large displacements between consecutive frames and numerous moving objects appearing in the scene.

According to Tab. 3, the proposed method is comparable with ORB-SLAM2. We summarize results of unsupervised learnable methods in Tab. 4. We show that our method significantly outperforms current state-of-the-art among all unsupervised deep learning-based approaches to trajectory estimation.

4.5. Results on EuRoC

For EuRoC dataset, we observed that it is more profitable to train visual odometry NN_{cons} on a mixture of strides 1, 2, 3, rather than training on a single stride. Results of NN_{cons} and NN_{loops} are presented in Tab. 5 for supervised training and in Tab. 6 for unsupervised training. We expected the results on EuRoC to resemble KITTI results, where supervised method surpasses unsupervised method remarkably. Surprisingly, metrics for our SLAM model trained in supervised and unsupervised manner are nearly the same. We attribute this to the following reasons. Firstly, since EuRoC scenes are rigid, generated flow looks similar to estimated flow. Secondly, randomly sampled training data prevent unsupervised method from overfitting, while supervised method tends to memorize the entire dataset.

Method	val ATE	val RPE_t	val RPE_r	test ATE	test RPE_t	test RPE_r
NN_{1+2+3}	1.35 ± 0.07	3.16 ± 0.20	19.75 ± 1.20	1.32 ± 0.06	2.78 ± 0.25	55.76 ± 2.16
NN_{loops}	1.43 ± 0.11	3.64 ± 0.30	23.88 ± 4.78	1.36 ± 0.05	3.02 ± 0.13	53.45 ± 2.00
SLAM	0.51 ± 0.015	1.06 ± 0.03	8.36 ± 0.17	0.81 ± 0.01	1.51 ± 0.02	19.59 ± 1.37

Table 5: Results of supervised visual odometry models and SLAM method on EuRoC dataset. Optimal parameters for SLAM are $C_{s_i} = 10000$, $C_r = 0.001$, $T_{loop} = 100$

Method	val ATE	val RPE_t	val RPE_r	test ATE	test RPE_t	test RPE_r
NN_{1+2+3}	1.06 ± 0.04	2.26 ± 0.14	20.97 ± 1.39	1.35 ± 0.46	3.04 ± 0.35	62.56 ± 3.29
NN_{loops}	1.37 ± 0.12	4.23 ± 0.59	33.49 ± 1.73	1.28 ± 0.05	3.43 ± 0.16	67.17 ± 4.36
SLAM	0.57 ± 0.008	1.12 ± 0.03	9.03 ± 0.20	0.84 ± 0.17	1.49 ± 0.27	23.13 ± 7.40

Table 6: Results of unsupervised visual odometry models and SLAM method on EuRoC dataset. Optimal parameters for SLAM are $C_{s_i} = 1000$, $C_r = 0.0001$, $T_{loop} = 100$

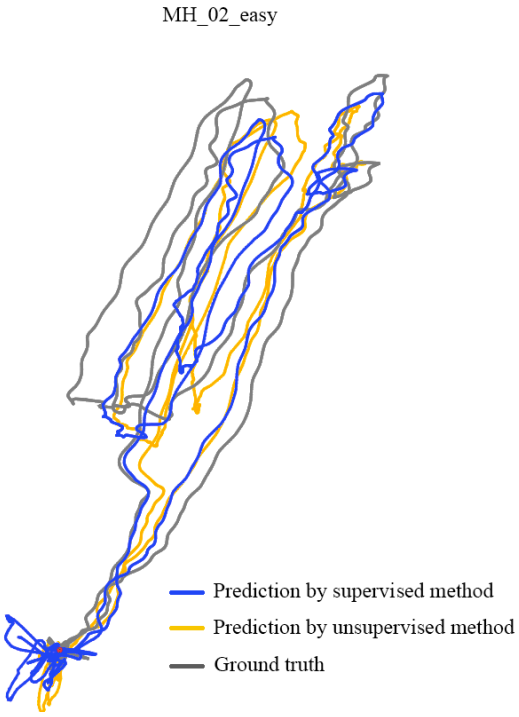


Figure 6: Ground truth and estimated EuRoC trajectory

5. Conclusion

We proposed an unsupervised method of training visual odometry and SLAM models on synthetic optical flow generated from depth map and arbitrary camera movement between selected real frame and virtual frame. This approach does not use frame sequences for training and does not require ground truth camera poses.

We also presented a simple way to build SLAM system from an arbitrary visual odometry model. To prove our ideas, we conducted experiments of training unsupervised SLAM on KITTI and EuRoC datasets. The implemented method demonstrated state-of-the-art results on KITTI dataset among unsupervised methods and showed robust performance on EuRoC. To the best of our knowledge, our visual odometry method is a pioneer work to train deep learning-base model on EuRoC in an unsupervised mode.

References

[1] Y. Almalioglu, M. R. U. Saputra, P. P. de Gusmao, A. Markham, and N. Trigoni. Ganvo: Unsupervised deep monocular visual odometry and depth estimation with generative adversarial networks. *arXiv preprint arXiv:1809.05786*, 2018. 1

[2] J.-W. Bian, Z. Li, N. Wang, H. Zhan, C. Shen, M.-M. Cheng, and R. I. Unsupervised scale-consistent depth and ego-motion learning from monocular video. *arXiv preprint arXiv:1908.10553*, 2019. 1, 6

[3] J.-L. Blanco, F.-A. Moreno, and J. González. A collection of outdoor robotic datasets with centimeter-accuracy ground truth. *Autonomous Robots*, 27(4):327–351, November 2009. 1

[4] G. Bradski. The OpenCV Library. *Dr. Dobb's Journal of Software Tools*, 2000. 3

[5] D. J. Butler, J. Wulff, G. B. Stanley, and M. J. Black. A naturalistic open source movie for optical flow evaluation. In A. Fitzgibbon et al. (Eds.), editor, *European Conf. on Computer Vision (ECCV)*, Part IV, LNCS 7577, pages 611–625. Springer-Verlag, Oct. 2012. 2

[6] J. L. B. Claraco. A tutorial on se3 transformation parameterizations and on-manifold optimization. Technical Report 012010, 2010. 4

[7] G. Costante and T. A. Ciarfuglia. Ls-vo: Learning dense optical subspace for robust visual odometry estimation. *IEEE Robotics and Automation Letters*, 3(3):1735–1742, 2018. 2, 6

[8] T. Dharmasiri, A. Spek, and T. Drummond. Eng: End-to-end neural geometry for robust depth and pose estimation using cnns. *arXiv preprint arXiv:1807.05705*, 2018. 2

[9] A. Dosovitskiy, P. Fischer, E. Ilg, P. Hausser, C. Hazirbas, V. Golkov, P. Van Der Smagt, D. Cremers, and T. Brox. Flownet: Learning optical flow with convolutional networks. In *Proceedings of the IEEE International Conference on Computer Vision*, pages 2758–2766, 2015. 2

[10] J. Engel, V. Koltun, and D. Cremers. Direct sparse odometry. *IEEE transactions on pattern analysis and machine intelligence*, 40(3):611–625, 2018. 2

[11] T. Feng and D. Gu. SGANVO: unsupervised deep visual odometry and depth estimation with stacked generative adversarial networks. *CoRR*, abs/1906.08889, 2019. 1, 6

[12] A. Geiger, P. Lenz, and R. Urtasun. Are we ready for autonomous driving? the kitti vision benchmark suite. In *Conference on Computer Vision and Pattern Recognition (CVPR)*, 2012. 1

[13] M. Geng, S. Shang, B. Ding, H. Wang, P. Zhang, and L. Zhang. Unsupervised learning-based depth estimation aided visual SLAM approach. *CoRR*, abs/1901.07288, 2019. 2

[14] J. F. Henriques and A. Vedaldi. Mapnet: An allocentric spatial memory for mapping environments. In *The IEEE Conference on Computer Vision and Pattern Recognition (CVPR)*, June 2018. 1

[15] C. Kerl, J. Sturm, and D. Cremers. Robust odometry estimation for rgb-d cameras. In *Robotics and Automation (ICRA), 2013 IEEE International Conference on*, pages 3748–3754. IEEE, 2013. 2

[16] R. Kuemmerle, G. Grisetti, H. Strasdat, K. Konolige, and W. Burgard. g2o: A general framework for graph optimization. In *Proceedings of the IEEE International Conference on Robotics and Automation (ICRA)*, pages 3607–3613, Shanghai, China, May 2011. 4

[17] R. Li, S. Wang, Z. Long, and D. Gu. Undeepvo: Monocular visual odometry through unsupervised deep learning. *CoRR*, abs/1709.06841, 2017. 1, 6

[18] D. G. Lowe. Distinctive image features from scale-invariant keypoints. *International Journal of Computer Vision*, 60(2):91–110, Nov 2004. 3

[19] D. G. Lowe, D. G. Lowe, and D. G. Lowe. Object recognition from local scale-invariant features. In *Proceedings of the International Conference on Computer Vision-Volume 2 - Volume 2*, ICCV '99, pages 1150–, Washington, DC, USA, 1999. IEEE Computer Society. 3

[20] Z. Lv, K. Kim, A. Troccoli, D. Sun, J. Rehg, and J. Kautz. Learning rigidity in dynamic scenes with a moving camera for 3d motion field estimation. In *ECCV*, 2018. 6

[21] R. Mahjourian, M. Wicke, and A. Angelova. Unsupervised learning of depth and ego-motion from monocular video using 3d geometric constraints. In *Proceedings of the IEEE Conference on Computer Vision and Pattern Recognition*, pages 5667–5675, 2018. 6

[22] N. Mayer, E. Ilg, P. Häusser, P. Fischer, D. Cremers, A. Dosovitskiy, and T. Brox. A large dataset to train convolutional networks for disparity, optical flow, and scene flow estimation. In *IEEE International Conference on Computer Vision and Pattern Recognition (CVPR)*, 2016. arXiv:1512.02134. 2

[23] M. Menze, C. Heipke, and A. Geiger. Object scene flow. *ISPRS Journal of Photogrammetry and Remote Sensing (JPRS)*, 2018. 2

[24] R. Mur-Artal and J. D. Tardós. Orb-slam2: An open-source slam system for monocular, stereo, and rgb-d cameras. *IEEE Transactions on Robotics*, 33(5):1255–1262, 2017. 2, 5

[25] T. Schops, T. Sattler, and M. Pollefeys. Bad slam: Bundle adjusted direct rgb-d slam. In *The IEEE Conference on Computer Vision and Pattern Recognition (CVPR)*, June 2019. 2

[26] I. Slinko, A. Vorontsova, F. Konokhov, O. Barinova, and A. Konushin. Scene motion decomposition for learnable visual odometry. *CoRR*, abs/1907.07227, 2019. 2

[27] F. Steinbrücker, J. Sturm, and D. Cremers. Real-time visual odometry from dense rgb-d images. In *Computer Vision Workshops (ICCV Workshops), 2011 IEEE International Conference on*, pages 719–722. IEEE, 2011. 2

[28] D. Sun, X. Yang, M.-Y. Liu, and J. Kautz. Pwc-net: Cnns for optical flow using pyramid, warping, and cost volume. In *Proceedings of the IEEE Conference on Computer Vision and Pattern Recognition*, pages 8934–8943, 2018. 2, 3

[29] Z. Teed and J. Deng. Deepv2d: Video to depth with differentiable structure from motion. *CoRR*, abs/1812.04605, 2018. 1, 2

[30] B. Ummenhofer, H. Zhou, J. Uhrig, N. Mayer, E. Ilg, A. Dosovitskiy, and T. Brox. Demon: Depth and motion network for learning monocular stereo. In *IEEE Conference on computer vision and pattern recognition (CVPR)*, volume 5, page 6, 2017. 2

[31] S. Vijayanarasimhan, S. Ricco, C. Schmid, R. Sukthankar, and K. Fragkiadaki. Sfm-net: Learning of structure and motion from video. *CoRR*, abs/1704.07804, 2017. 1, 2

[32] S. Wang, R. Clark, H. Wen, and N. Trigoni. Deepvo: Towards end-to-end visual odometry with deep recurrent convolutional neural networks. In *Robotics and Automation (ICRA), 2017 IEEE International Conference on*, pages 2043–2050. IEEE, 2017. 1, 2, 6

[33] S. Wang, R. Clark, H. Wen, and N. Trigoni. End-to-end, sequence-to-sequence probabilistic visual odometry through deep neural networks. *The International Journal of Robotics Research*, 37(4-5):513–542, 2018. 1

[34] S. Wang, R. Clark, H. Wen, and N. Trigoni. End-to-end, sequence-to-sequence probabilistic visual odometry through deep neural networks. *The International Journal of Robotics Research*, 37(4-5):513–542, 2018. 2

[35] F. Xue, X. Wang, S. Li, Q. Wang, J. Wang, and H. Zha. Beyond tracking: Selecting memory and refining poses for deep visual odometry. In *The IEEE Conference on Computer Vision and Pattern Recognition (CVPR)*, June 2019. 1

[36] Z. Yin and J. Shi. Geonet: Unsupervised learning of dense depth, optical flow and camera pose. In *Proceedings of the IEEE Conference on Computer Vision and Pattern Recognition (CVPR)*, volume 2, 2018. 1, 6

[37] J. Zbontar and Y. LeCun. Stereo matching by training a convolutional neural network to compare image patches. *CoRR*, abs/1510.05970, 2015. 3

[38] H. Zhan, R. Garg, C. S. Weerasekera, K. Li, H. Agarwal, and I. D. Reid. Unsupervised learning of monocular depth estimation and visual odometry with deep feature reconstruction. *CoRR*, abs/1803.03893, 2018. 1, 6

[39] H. Zhan, C. S. Weerasekera, J. Bian, and I. Reid. Visual odometry revisited: What should be learnt? *arXiv preprint arXiv:1909.09803*, 2019. 5, 6

[40] C. Zhao, L. Sun, P. Purkait, T. Duckett, and R. Stolkin. Learning monocular visual odometry with dense 3d mapping from dense 3d flow. *Intelligent Robots and Systems (IROS), 2018 International Conference on*, 2018. 6

[41] H. Zhou, B. Ummenhofer, and T. Brox. Deeptam: Deep tracking and mapping. In *European Conference on Computer Vision (ECCV)*, 2018. 1, 2, 6

[42] T. Zhou, M. Brown, N. Snavely, and D. G. Lowe. Unsupervised learning of depth and ego-motion from video. In *CVPR*, volume 2, page 7, 2017. 1, 2, 6

Training Deep SLAM on Single Frames
— Supplementary Material —

1. Optical flow synthesis

We provide several examples of synthesized and estimated optical flow (OF) for KITTI dataset on Figure 1 and for EuRoC dataset on Figure 2. It can be observed that estimated OF is more cluttered compared to synthesized OF, while synthesized OF is more smooth.

2. Detailed description of experiments

We present detailed comparison of our method with other deep learning-based monocular visual odometry and SLAM methods on KITTI. We report results on sequences 03, 04, 05, 06, 07, 10 (Figure 3) which are commonly used for evaluation. We train our network for 5 times and report the average values for translation error t_{err}, rotation error r_{err} and ATE. Since sequences 03, 04, 10 do not contain loops, the results of our visual odometry and SLAM models do not differ.

Unsupervised methods. Results for each of the sequences 03, 04, 05, 06, 07, 10 are shown in Table 3. Overall, our visual odometry outperforms listed unsupervised methods. It shows better results than SGANVO[3] on sequences 03 and 10 and performs at the same level on sequences 05 and 06. According to Table 3, adding graph optimization helps to improve results for trajectories with loops. Thus, we believe that our method of converting visual odometry model to SLAM system can be used along with standard unsupervised learning pipeline.

Supervised methods. We evaluate our visual odometry and SLAM against supervised methods on sequences 03, 04, 05, 06, 07, 10 from KITTI. The results are reported in Table 4. While our model is quite simple and accounts only for pairs of similar frames, it outperforms more complex models. This may indicate that not the choice of proper network architecture, but the lack of training data is the major difficulty when developing a trainable visual odometry method. Therefore, in our work we address this issue rather than focus on improving the network architecture.

Pose graphs visualization. Figure 5 shows the graphs that were used for optimization. Here blue edges correspond to consecutive frames and orange edges correspond to detected loops.

6DoF	NN_{cons}		NN_{loops}	
	$\mu, 10^{-2}$	$\sigma, 10^{-2}$	$\mu, 10^{-2}$	$\sigma, 10^{-2}$
x	-0.01	2.64	1.54	20.31
y	-1.72	1.88	-3.41	32
z	92.19	29.77	139.6	131
$euler_x$	0	0.3	0.03	0.62
$euler_y$	0.07	1.83	0.28	6.39
$euler_z$	0	0.28	0.01	0.63

Table 1: Parameters of t-distributions with $\nu = 4$ degrees of freedom that were used to approximate motions on KITTI dataset. μ and σ for x, y, z are in meters and for $euler_x, euler_y, euler_z$ are in radians

6DoF	NN_{cons}		NN_{loops}	
	$\mu, 10^{-3}$	$\sigma, 10^{-2}$	$\mu, 10^{-3}$	$\sigma, 10^{-2}$
x	4.2	2.6	17.8	12.8
y	-3.26	5.56	17.2	21.6
z	8.49	3.26	50	29.2
$euler_x$	-1.03	2.26	-1.9	12
$euler_y$	0.354	1.77	0.69	3.9
$euler_z$	0.391	1.54	-1.6	5.4

Table 2: Parameters of t-distributions with $\nu = 4$ degrees of freedom that were used to approximate motions on EuRoC dataset. μ and σ for x, y, z are in meters and for $euler_x, euler_y, euler_z$ are in radians

3. Additional ablation studies

Error analysis for monocular visual odometry. To analyse distribution of the errors of supervised visual odometry we plot the values of error with respect to the distance traveled. These plots are showed in Figure 6. We show errors for consecutive frames (with NN_{cons}) and for loops (with NN_{loops}). One can notice that the errors of the NN_{loops} are significantly larger than the errors for consecutive frames, and overall the larger is the magnitude of the motion, the larger is the error.

[2]the updated model in Github is evaluated

[2]currently the top monocular method on KITTI test

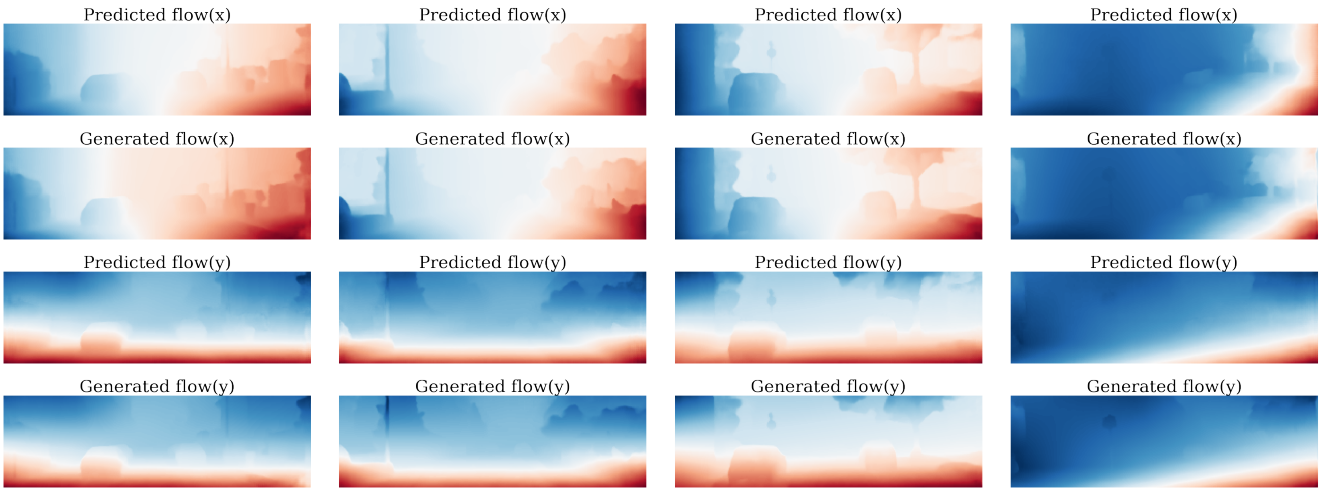


Figure 1: Examples of predicted optical flow with PWC-net[6] and synthesised optical flow for KITTI dataset

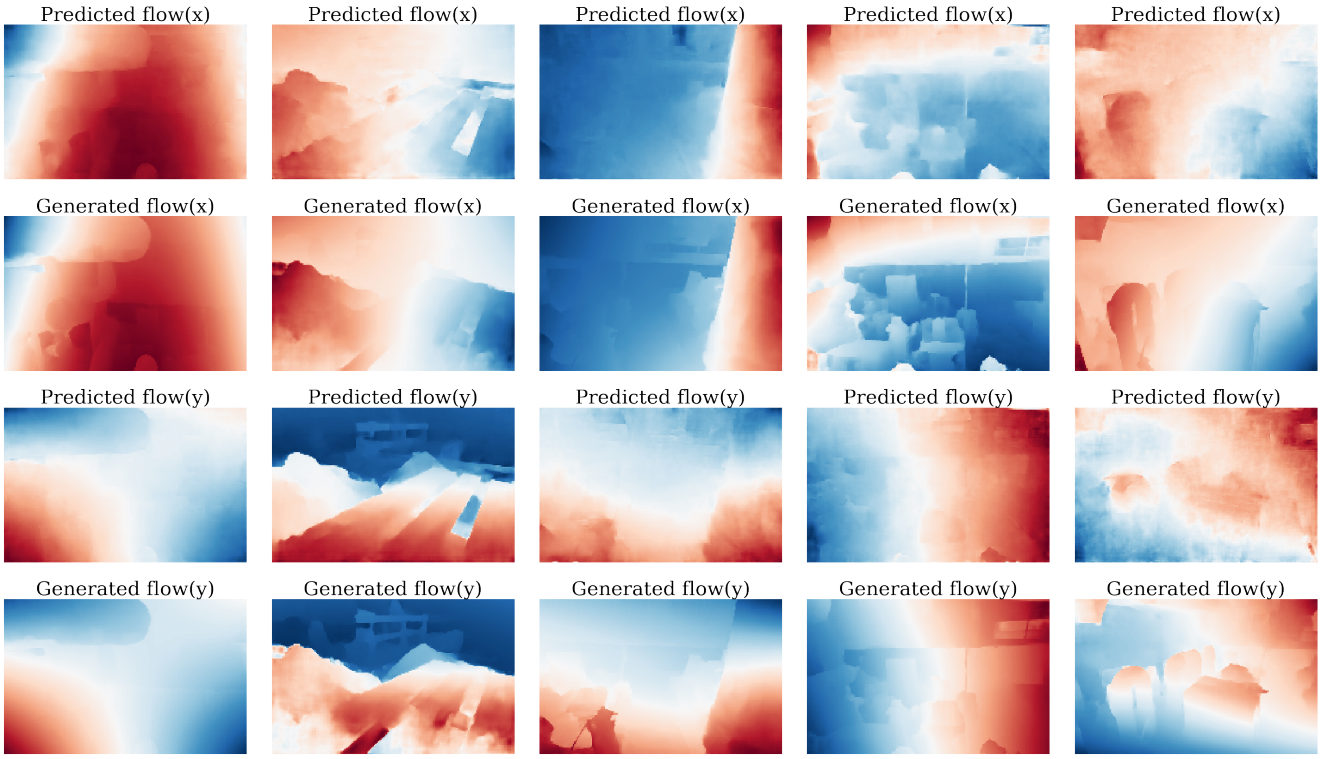


Figure 2: Examples of predicted optical flow with PWC-net[6] and synthesised optical flow for EuRoC dataset

Analysis of motion distribution. We analyse the joint distributions for all pairs of motion components between consecutive frames on KITTI and EuRoC datasets in Figure 7 and Figure 8 respectively. Figures shows the 2d distribution plots. We approximate 6DoF with 6 independent t-distributions. Estimated parameters for these distributions are listed in Table 1 for KITTI dataset and in Table 2 for EuRoC dataset. We also plot the motions sampled from the t-distribution used in our experiments. It can be seen that in most cases the synthetic samples and real samples appear in very similar locations.

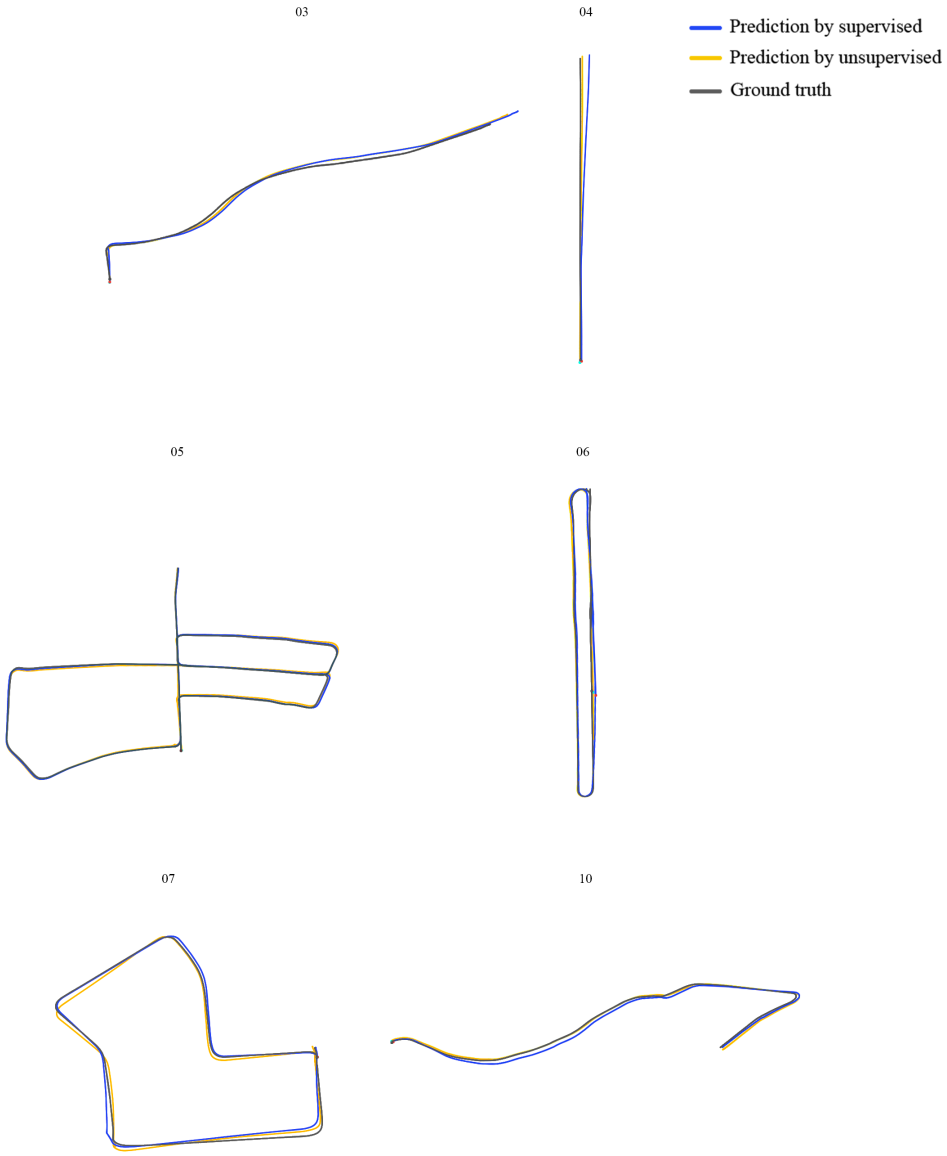


Figure 3: 03, 04, 05, 06, 07, 10 sequences of KITTI dataset predicted by our supervised and unsupervised SLAM models.

Method	Metric	03	04	05	06	07	10	Avg
SfMLearner[14] [1]	t_{err}	12.56	4.32	12.99	15.55	12.61	15.25	12.21
	r_{err}	<u>4.52</u>	3.28	4.66	5.58	6.31	4.06	4.74
	ATE	8.42	3.10	60.89	52.19	20.12	24.09	28.14
Depth-VO-Feat[12]	t_{err}	15.76	3.14	4.94	5.80	6.49	12.82	8.15
	r_{err}	10.62	2.02	2.34	2.06	3.56	3.41	4.00
	ATE	21.34	3.12	22.15	14.31	15.35	24.70	16.83
SC-SfMLearner[1]	t_{err}	9.22	4.22	6.70	5.36	8.29	10.74	7.42
	r_{err}	4.93	2.01	2.38	1.65	4.53	4.58	3.35
	ATE	10.21	2.97	40.56	12.56	21.01	20.19	17.92
UnDeepVO[4]	t_{err}	<u>5.00</u>	5.49	3.40	6.20	3.15	10.63	5.65
	r_{err}	6.17	2.13	1.50	1.98	2.48	4.65	3.15
GeoNet[11]	t_{err}	19.21	9.09	20.12	9.28	8.27	20.73	13.12
	r_{err}	9.78	7.54	7.67	4.34	5.93	9.04	7.38
Vid2Depth[5]	t_{err}	27.12	18.92	51.13	58.07	51.22	21.54	37.98
	r_{err}	10.39	1.19	21.86	26.83	36.64	12.54	18.24
SGANVO[3] [2]	t_{err}	10.56	**2.40**	3.25	**3.99**	**4.67**	5.89	<u>5.12</u>
	r_{err}	6.30	**0.77**	1.31	1.46	**1.83**	3.56	2.53
Ours (unsup) VO	t_{err}	**2.98**	12.70	4.64	5.81	13.28	**3.99**	5.57
	r_{err}	**0.93**	1.72	1.68	1.68	8.76	**1.13**	<u>2.23</u>
	ATE	1.08	2.08	18.53	14.25	4.64	5.20	14.30
Ours (unsup) SLAM	t_{err}	**2.98**	12.70	**2.15**	4.07	7.24	**3.99**	**3.37**
	r_{err}	**0.93**	1.72	**0.81**	**0.86**	4.41	**1.13**	**1.24**
	ATE	1.08	2.08	2.62	3.69	5.18	5.20	**3.24**

Table 3: Results of unsupervised deep learning-based methods on test trajectories from KITTI dataset. The best results are shown in bold. The second best is underlined.

Method	Metric	03	04	05	06	07	10	Avg
2D-Flow[13]	t_{err}	3.35	4.15	2.49	3.19	17.20	7.24	6.27
	r_{err}	1.62	2.53	1.19	1.54	10.40	3.06	3.39
3D-Flow[13]	t_{err}	**3.18**	2.04	2.59	1.39	2.81	4.38	2.73
	r_{err}	**1.31**	0.81	0.99	0.95	2.54	3.12	1.62
DeepVO[7]	t_{err}	8.49	7.19	2.62	5.42	3.91	8.11	5.96
	r_{err}	6.89	6.97	3.61	5.82	4.60	8.83	6.12
ESP-VO[8]	t_{err}	6.72	6.33	3.35	7.24	3.52	9.77	6.15
	r_{err}	6.46	6.08	4.93	7.29	5.02	10.20	6.63
$SRNN_{channel}$[9]	t_{err}	5.44	2.91	3.27	8.50	3.37	6.32	4.80
	r_{err}	3.32	1.30	1.62	2.74	2.25	2.33	2.26
LS-VO[2]	t_{err}	5.30	**0.78**	2.36	2.91	3.51	3.31	2.54
	r_{err}	1.53	**0.42**	0.91	1.14	5.53	1.26	1.80
SMRP[10]	t_{err}	3.32	2.96	2.59	4.93	**3.07**	3.94	3.47
	r_{err}	2.10	1.76	1.25	1.90	**1.76**	1.72	1.75
Ours (sup) VO	t_{err}	4.23	4.42	1.43	1.97	4.48	**2.01**	<u>2.07</u>
	r_{err}	1.70	1.08	0.60	0.77	2.89	**0.74**	<u>0.93</u>
	ATE	1.57	1.01	5.53	7.21	7.35	2.53	<u>4.38</u>
Ours (sup) SLAM	t_{err}	4.23	4.42	**0.86**	**1.05**	3.58	**2.01**	**1.54**
	r_{err}	1.70	1.08	**0.38**	**0.44**	2.49	**0.74**	**0.74**
	ATE	1.57	1.01	1.52	1.33	3.36	2.53	**1.84**

Table 4: Results of supervised deep-learning-based methods on test trajectories from KITTI dataset. The best results are shown in bold. The second best is underlined.

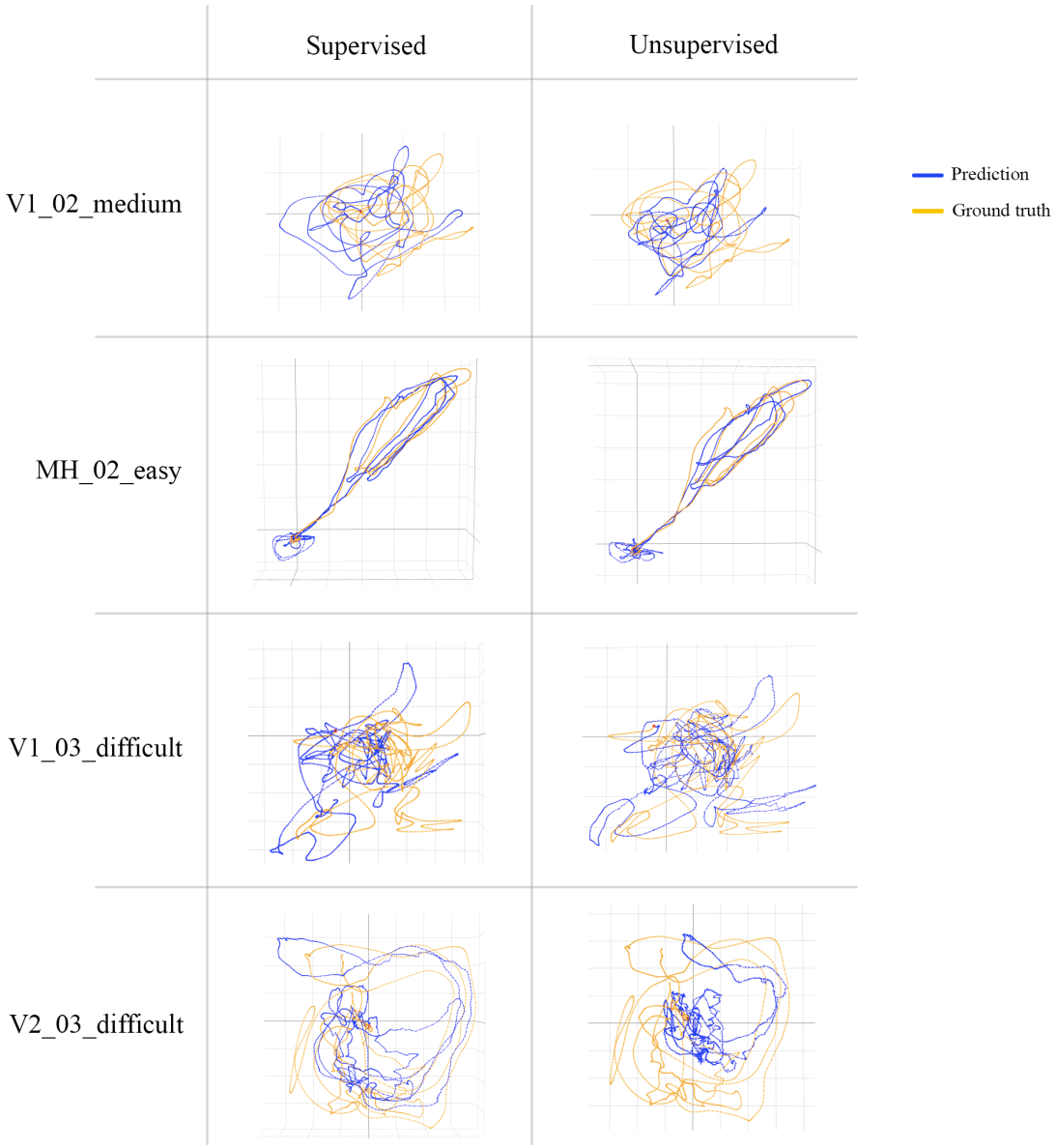


Figure 4: Predicted trajectories for V1_02_medium, MH_02_easy, V1_03_difficult, V2_03_difficult sequences of EuRoC dataset by our supervised and unsupervised SLAM models.

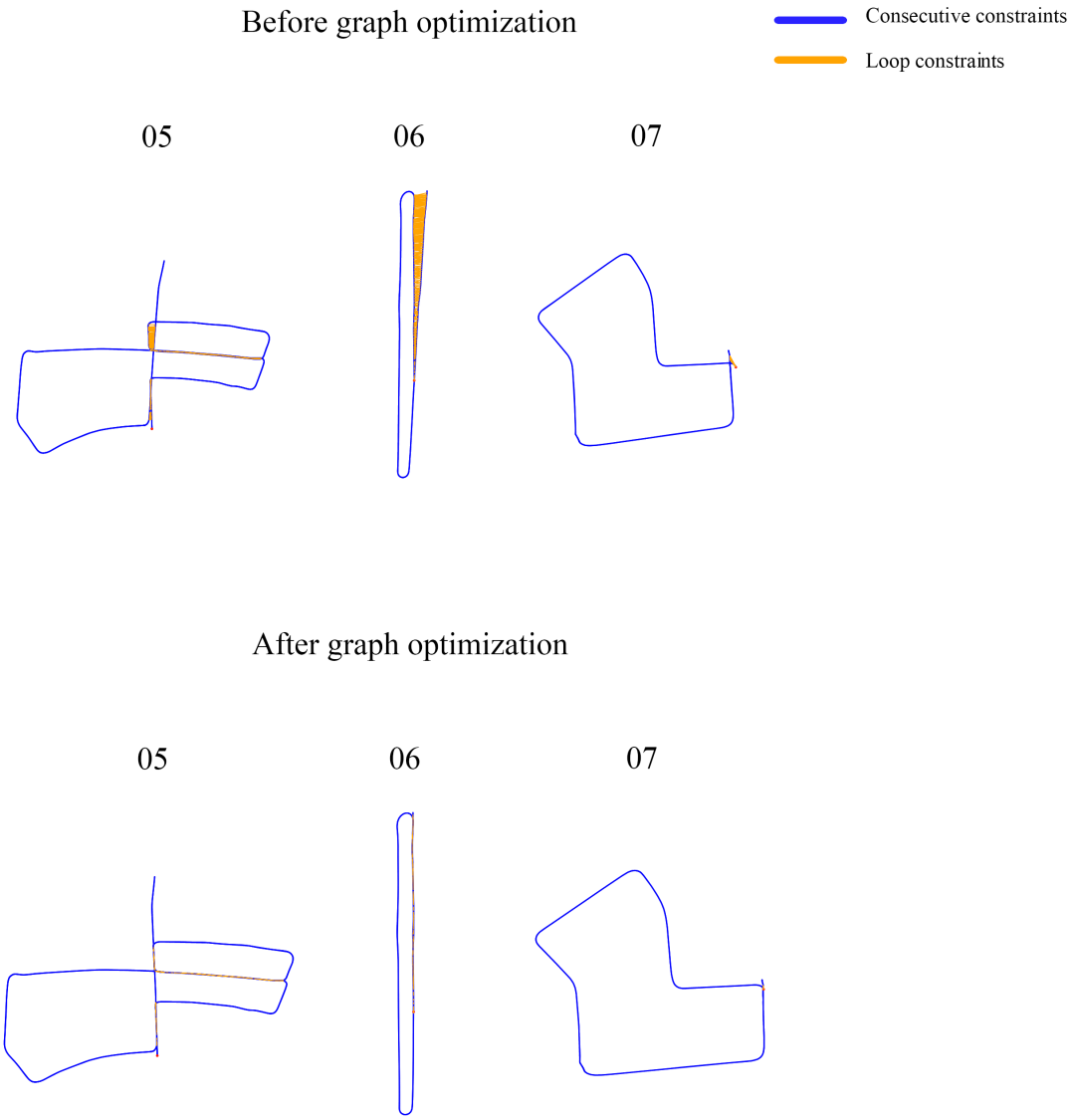


Figure 5: Pose graphs for trajectories from KITTI. The edges connect either consecutive frames or the pairs of frames where loop closure was detected. The first type of links in a graph is shown in blue. The second type of links is shown in orange.

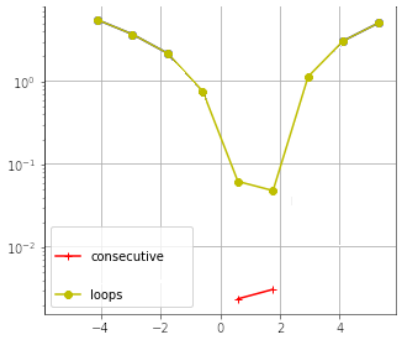


Figure 6: Errors of supervised visual odometry with respect to magnitude of the motion on KITTI dataset.

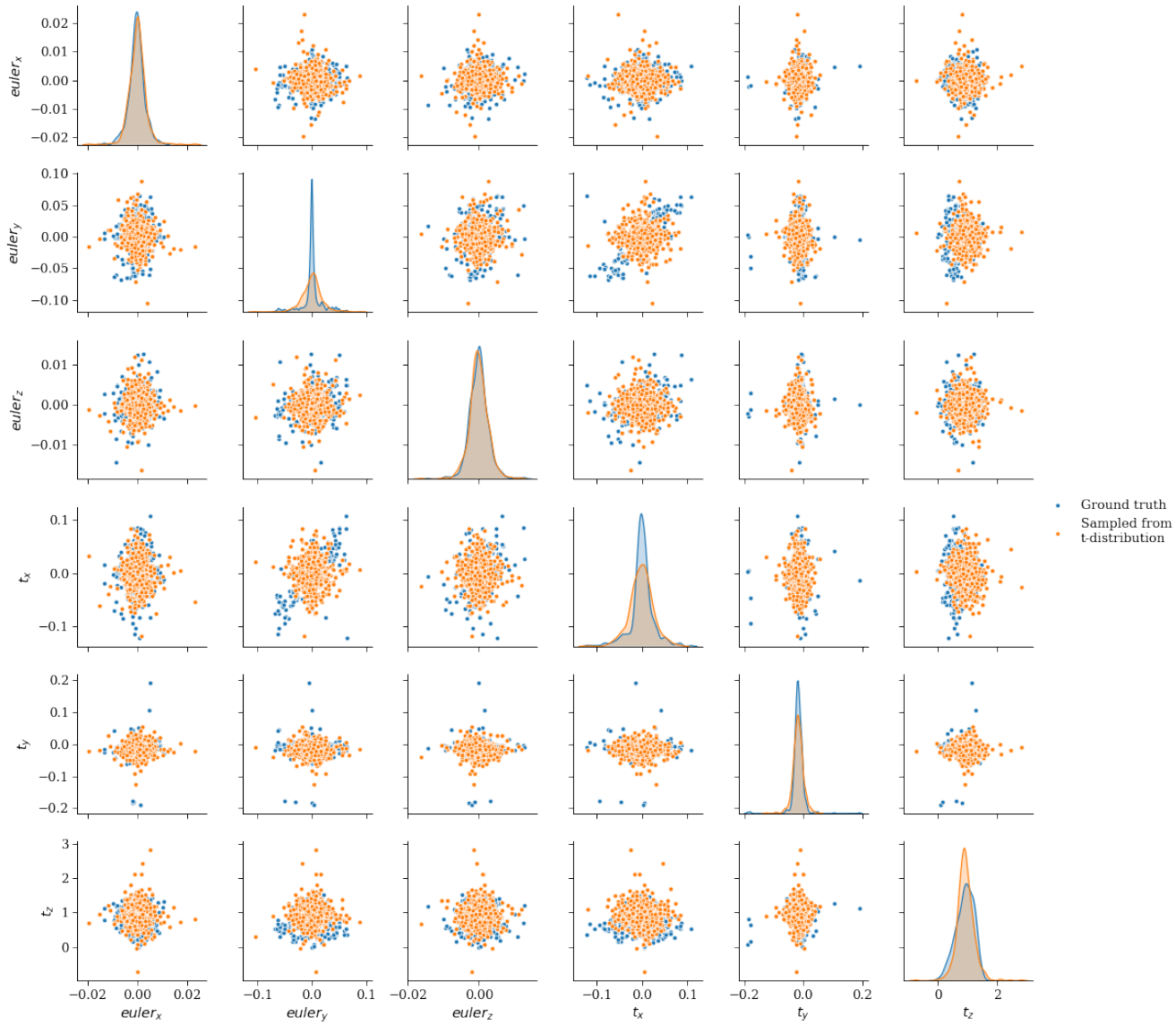


Figure 7: Motion distributions for training NN_{cons} on KITTI dataset. The subplots show pairwise joint distributions for all pairs of the motion components (Euler angles x, y, z and translations x, y, z). Blue dots are real samples and orange dots are synthetic samples.

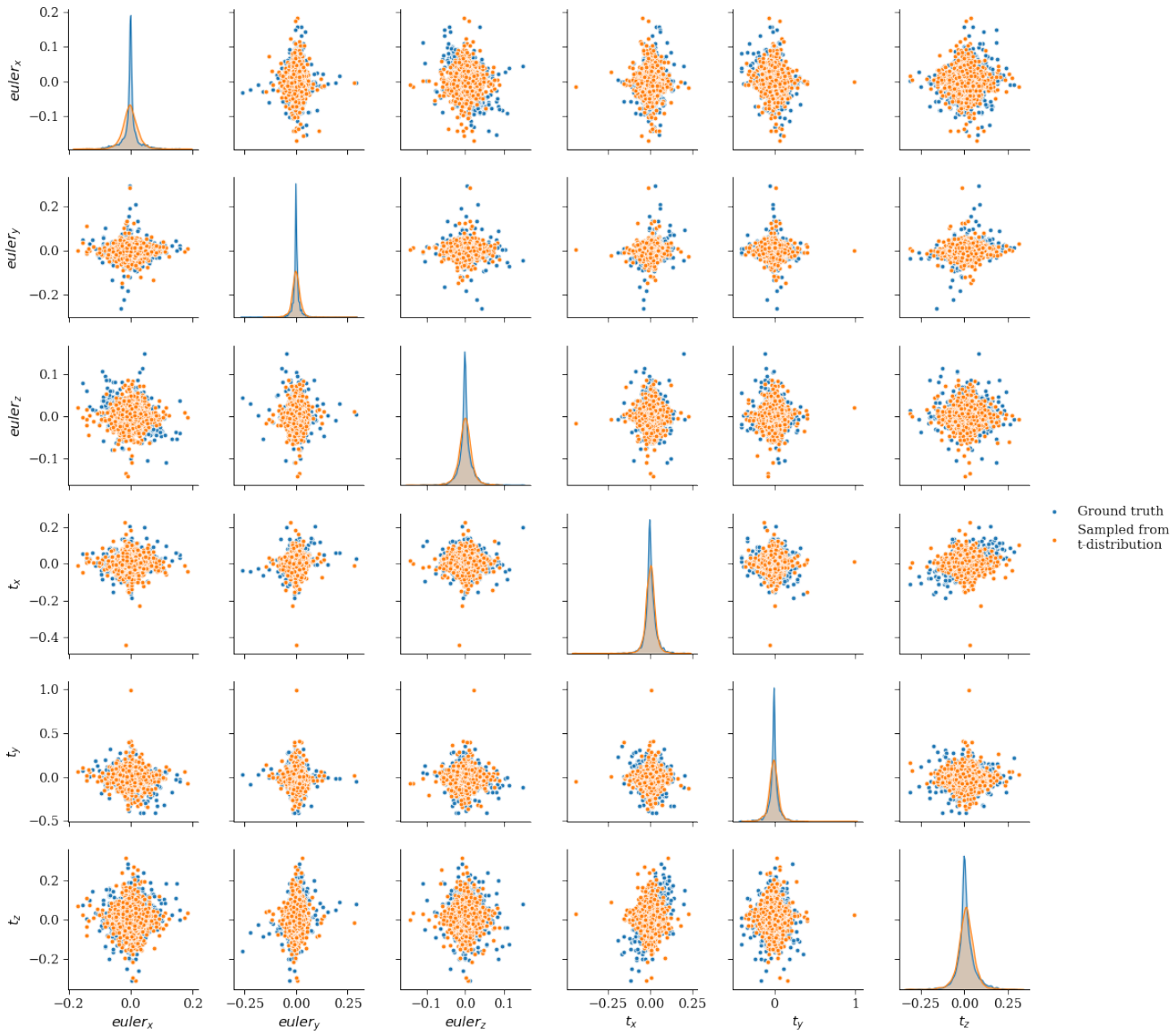


Figure 8: Motion distributions for training NN_{cons} on EuRoC dataset. The subplots show pairwise joint distributions for all pairs of the motion components (Euler angles x, y, z and translations x, y, z). Blue dots are real samples and orange dots are synthetic samples.

References

[1] J.-W. Bian, Z. Li, N. Wang, H. Zhan, C. Shen, M.-M. Cheng, and R. I. Unsupervised scale-consistent depth and ego-motion learning from monocular video. *arXiv preprint arXiv:1908.10553*, 2019. 4

[2] G. Costante and T. A. Ciarfuglia. LS-VO: learning dense optical subspace for robust visual odometry estimation. *CoRR*, abs/1709.06019, 2017. 4

[3] T. Feng and D. Gu. SGANVO: unsupervised deep visual odometry and depth estimation with stacked generative adversarial networks. *CoRR*, abs/1906.08889, 2019. 1, 4

[4] R. Li, S. Wang, Z. Long, and D. Gu. Undeepvo: Monocular visual odometry through unsupervised deep learning. *CoRR*, abs/1709.06841, 2017. 4

[5] R. Mahjourian, M. Wicke, and A. Angelova. Unsupervised learning of depth and ego-motion from monocular video using 3d geometric constraints. In *Proceedings of the IEEE Conference on Computer Vision and Pattern Recognition*, pages 5667–5675, 2018. 4

[6] D. Sun, X. Yang, M.-Y. Liu, and J. Kautz. Pwc-net: Cnns for optical flow using pyramid, warping, and cost volume. In *Proceedings of the IEEE Conference on Computer Vision and Pattern Recognition*, pages 8934–8943, 2018. 2

[7] S. Wang, R. Clark, H. Wen, and N. Trigoni. Deepvo: Towards end-to-end visual odometry with deep recurrent convolutional neural networks. In *Robotics and Automation (ICRA), 2017 IEEE International Conference on*, pages 2043–2050. IEEE, 2017. 4

[8] S. Wang, R. Clark, H. Wen, and N. Trigoni. End-to-end, sequence-to-sequence probabilistic visual odometry through deep neural networks. *The International Journal of Robotics Research*, 37(4-5):513–542, 2018. 4

[9] F. Xue, Q. Wang, X. Wang, W. Dong, J. Wang, and H. Zha. Guided feature selection for deep visual odometry. *CoRR*, abs/1811.09935, 2018. 4

[10] F. Xue, X. Wang, S. Li, Q. Wang, J. Wang, and H. Zha. Beyond tracking: Selecting memory and refining poses for deep visual odometry. In *The IEEE Conference on Computer Vision and Pattern Recognition (CVPR)*, June 2019. 4

[11] Z. Yin and J. Shi. Geonet: Unsupervised learning of dense depth, optical flow and camera pose. In *Proceedings of the IEEE Conference on Computer Vision and Pattern Recognition (CVPR)*, volume 2, 2018. 4

[12] H. Zhan, R. Garg, C. S. Weerasekera, K. Li, H. Agarwal, and I. D. Reid. Unsupervised learning of monocular depth estimation and visual odometry with deep feature reconstruction. *CoRR*, abs/1803.03893, 2018. 4

[13] C. Zhao, L. Sun, P. Purkait, T. Duckett, and R. Stolkin. Learning monocular visual odometry with dense 3d mapping from dense 3d flow. *Intelligent Robots and Systems (IROS), 2018 International Conference on*, 2018. 4

[14] T. Zhou, M. Brown, N. Snavely, and D. G. Lowe. Unsupervised learning of depth and ego-motion from video. In *CVPR*, volume 2, page 7, 2017. 4